

# Particle size and composition distribution analysis of automotive brake abrasion dusts for the evaluation of antimony sources of airborne particulate matter

Akihiro Iijima<sup>a,\*</sup>, Keiichi Sato<sup>b</sup>, Kiyoko Yano<sup>c</sup>, Hiroshi Tago<sup>a</sup>, Masahiko Kato<sup>a</sup>, Hirokazu Kimura<sup>d</sup>, Naoki Furuta<sup>b</sup>

<sup>a</sup>Gunma Prefectural Institute of Public Health and Environmental Sciences, 378 Kamioki, Maebashi, Gunma 371-0052, Japan

<sup>b</sup>Department of Applied Chemistry, Faculty of Science and Engineering, Chuo University, 1-13-27 Kasuga, Bunkyo-ku, Tokyo 112-8551, Japan

<sup>c</sup>Akebono Brake Industry, Co., Ltd., 5-4-71 Higashi, Hanyu, Saitama 348-8509, Japan

<sup>d</sup>Infectious Diseases Surveillance Center, National Institute of Infectious Diseases, 4-7-1 Gakuen, Musashimurayama, Tokyo 208-0011, Japan

Received 18 October 2006; received in revised form 2 February 2007; accepted 3 February 2007

## Abstract

Abrasion dusts from three types of commercially available non-steel brake pads were generated by a brake dynamometer at disk temperatures of 200, 300 and 400 °C. The number concentration of the abrasion dusts and their aerodynamic diameters ( $D_p$ ) were measured by using an aerodynamic particle sizer (APS) spectrometer with high temporal and size resolution. Simultaneously, the abrasion dusts were also collected based on their size by using an Andersen low-volume sampler, and the concentrations of metallic elements (K, Ti, Fe, Cu, Zn, Sb and Ba) in the size-classified dusts were measured by ICP-AES and ICP-MS. The number distributions of the brake abrasion dusts had a peak at  $D_p$  values of 1 and 2  $\mu\text{m}$ ; this peak shifted to the coarse side with an increase in the disk temperature. The mass distributions calculated from the number distributions have peaks between  $D_p$  values of 3 and 6  $\mu\text{m}$ . The shapes of the elemental mass distributions (Ti, Fe, Cu, Zn, Sb and Ba) in size-classified dusts were very similar to the total mass distributions of the brake abrasion dusts. These experimental results indicated that the properties of brake abrasion dusts were consistent with the characteristics of Sb-enriched fine airborne particulate matter. Based on these findings and statistical data, the estimation of Sb emission as airborne particulate matter from friction brakes was also discussed.

© 2007 Elsevier Ltd. All rights reserved.

**Keywords:** Airborne particulate matter; PM<sub>2.5</sub>; Particle size distribution; Brake dust; Antimony

## 1. Introduction

The atmosphere contains airborne particulate matter (APM) of different sizes. Since fine particles with diameters of less than 2.5  $\mu\text{m}$  (PM<sub>2.5</sub>) enter the lungs during respiration and remain in their peripheries, they may cause an adverse effect on

\*Corresponding author. Tel.: +81 27 232 4881; fax: +81 27 234 8438.

E-mail address: [ijima-akihiro@pref.gunma.jp](mailto:ijima-akihiro@pref.gunma.jp) (A. Iijima).

human health (Calcabrini et al., 2004; Oberdoerster, 2005). According to an epidemiological study, there is a significant relationship between the concentration of PM<sub>2.5</sub> and human mortality (Borja-Aburto et al., 1998). It was reported that a 10 µg m<sup>-3</sup> increase in PM<sub>2.5</sub> would be associated with a 1.4% increase in mortality (Borja-Aburto et al., 1998). With regard to the respective chemical species, toxic substances with carcinogenicity and chronic toxicity, such as polycyclic aromatic hydrocarbons and toxic metallic elements, are found in PM<sub>2.5</sub> collected in an urban district (Gao et al., 2002; Lim et al., 2005). According to previous studies, there appears to be a significant relationship between these toxic substances and chronic diseases such as cardiopulmonary function failure, genotoxic hazard, and so on (Lippmann and Ito, 2000; Magari et al., 2002).

The results of the long-term monitoring of APM in Tokyo (Furuta et al., 2005) indicate that fine particles with a diameter of less than 2 µm are extremely enriched with antimony (Sb) when compared with crustal materials. Sb-enriched APM have also been observed in several countries, e.g. USA (Gao et al., 2002), Germany (Weckwerth, 2001) and Argentina (Gomez et al., 2005). Furthermore, Krachler et al. (2005) reported the increasing of atmospheric Sb contamination in the northern hemisphere from the observation of snow and ice core samples. In our previous study, particle shape could be morphologically classified into three types (spherical, cotton-like and edgy-shaped; typical images were shown in the paper (Furuta et al., 2005)), and the results of the composition analysis by SEM-EDX for single particle have revealed that a vast majority of edgy-shaped fine particles contain high concentrations of Sb. This observation suggests that such particles are produced by the mechanical abrasion of Sb-enriched materials. Some non-steel (non-asbestos organic) brake pads used in the disk brake system of an automobile contain Sb<sub>2</sub>S<sub>3</sub> as a solid lubricant that reduces the wear of friction materials under high load conditions (Jang and Kim, 2000). According to the morphological observation by using SEM, brake abrasion dusts were mainly edgy-shaped as we expected (Furuta et al., 2005). Hence, the brake abrasion dust generated by the friction brake of automobiles might be one of the possible sources of Sb-enriched APM (Weckwerth, 2001; Sternbeck et al., 2002; Pakkanen et al., 2003; Adachi and Tainosho, 2004; Lough et al., 2005; Furuta et al., 2005). In addition, Uexküll et al.

(2005) have suggested that some amount of Sb<sub>2</sub>S<sub>3</sub> could be oxidized to Sb<sub>2</sub>O<sub>3</sub>, one of the possible carcinogenic compounds, by frictional heating during braking (IARC, 1989). Thus, we should pay more attention to automotive brake abrasion dusts from the viewpoint of toxicology. However, few studies have investigated the physical or chemical properties of the brake abrasion dusts such as the particle size distributions and size-classified metallic element compositions. Garg et al. (2000) used a micro-orifice uniform deposit impactor (MOUDI) to demonstrate that some particle mass distributions of the brake abrasion dusts generated by a brake dynamometer installed in a closed chamber show a bimodal (aerodynamic diameter range <0.1 and >10 µm) profile. Sanders et al. (2003) have also used a MOUDI and reported that the particle mass distribution of the brake abrasion dusts generated by a brake dynamometer installed in an open system covered with a hood exhibits a peak at approximately 6 µm, which was considerably different from the results of Garg et al. (2000). However, no reports are available for the distributions of elemental concentrations (including Sb) in size-classified abrasion dusts. In order to demonstrate that brake abrasion dusts are one of the important Sb sources in fine APM, it is necessary to determine the particle size distribution of abrasion dusts and the elemental distribution in size-classified dusts emitted during the actual braking process.

In this study, we measured the aerodynamic particle size distributions of the brake abrasion dusts produced by a brake dynamometer; additionally, we analyzed the concentrations of metallic elements present in the size-classified abrasion dusts that were produced in the dynamometer abrasion tests. Moreover, the estimation of Sb emission from the automotive brake abrasion dusts is also discussed.

## 2. Experimental

### 2.1. Condition of abrasion test by the brake dynamometer

Three types of commercially available non-steel (non-asbestos organic) brake pads (described as A, B and C) made by different brake manufacturers in Japan were used for the abrasion tests. These pads are used in typical Japanese passenger cars and there are not so big differences in composition

among these three pads. The abrasion dusts were produced using a brake dynamometer. A cast iron disk was fixed on a rotating shaft, and a pair of brake pads was installed in a caliper. Both the iron disk and the brake pads were continuously cooled by an air flow with a wind velocity of  $3 \text{ m s}^{-1}$  from a blower mounted at 300 mm on the oblique upper part of the caliper, as shown in Fig. 1. The temperatures of the disk and pads were measured using a thermocouple attached at a depth of 1 mm from the friction surface. The test procedure based on JASO (Japanese Automotive Standard Organization)-C427-88 was used to generate the abrasion dusts.

The disk idly rotated at a constant speed and was then braked with a constant deceleration of  $3.0 \text{ m s}^{-2}$ . The particle size distribution was measured at disk temperatures of 200, 300 and 400 °C. The disk temperature of 200 °C is generally produced by braking during urban district driving (Sasaki et al., 1994). On the other hand, the disk temperatures of 300 and 400 °C are produced under high-load and extremely high-load conditions, respectively, such as those during downhill braking. At 200 and 300 °C, the initial speed of the disk rotation was set to  $50 \text{ km h}^{-1}$ , while at 400 °C, it was set to  $80 \text{ km h}^{-1}$ . Before beginning the abrasion

tests, the friction surface was burnished to eliminate roughness at the disk temperature of 200 °C. At the beginning of the abrasion tests, the temperature of the disk was raised from the room temperature to 200 °C by repetitive braking in a short interval, and the measurement of the particle size distribution started after the disk temperature had reached 200 °C. The disk and pads heated by braking were cooled by the air flow from a blower. They were subjected to further braking when the disk temperature reached 200 °C. The brakes were applied 20 times under identical conditions (they were applied 5 times at the beginning for achieving stabilization and 15 times thereafter for measuring the particle size distribution). Further tests were conducted by heating the disk to 300 and 400 °C by the procedure similar to that mentioned above. At each temperature, the braking and cooling were repeated 20 times.

## 2.2. Analysis of particle size distribution

The particle size distributions of the abrasion dusts were analyzed by using an aerodynamic particle sizer (APS) spectrometer (Model 3321 APS, Tokyo Dylec Co., Japan) (Kenny and Liden, 1991; Sioutas et al., 1999). In order to avoid the interaction between the abraded particles such as aggregation or deposition, the sample intake of the spectrometer was installed just 200 mm below the caliper in the tangential direction (Fig. 1). The particle size was calculated as the aerodynamic diameter ( $D_p$ ) from the time of flight for passing between two laser beams. Since the APS spectrometer has high signal response, it is possible to obtain the short-time profiles of particle size distribution. In this study, it was possible to measure the  $D_p$  and the number of abrasion dusts with a temporal resolution of 1 s and a size resolution of 52 classes in the range of  $D_p = 0.5\text{--}20 \mu\text{m}$ .

## 2.3. Collection of size-classified abrasion dust samples for elemental analysis

In order to confirm the elemental distribution in size-classified abrasion dusts, brake abrasion dusts were collected depending on their size by using the Andersen low-volume sampler (AN-200, Tokyo Dylec Co.); simultaneously, the particle size distributions were measured using the APS spectrometer. The sample intake of the sampler was set

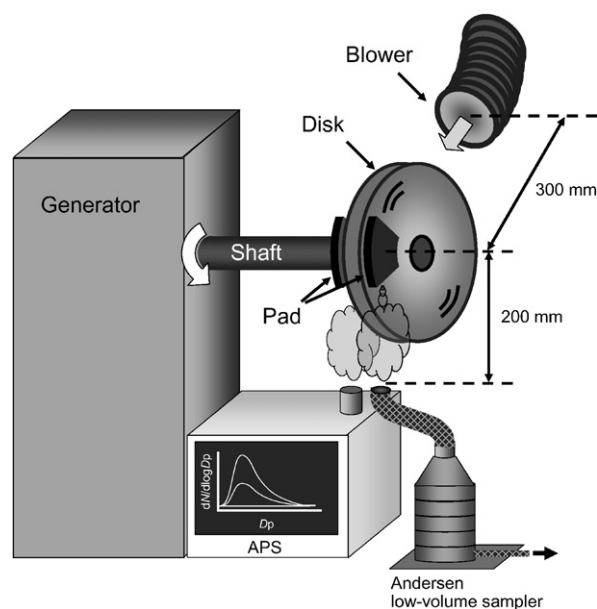


Fig. 1. Layout of full size brake dynamometer and measurement instruments.

adjacent to the APS intake (Fig. 1). The abrasion dusts were collected on a quartz fiber filter (2500 QAT-UP, Pallflex Products Co., USA) with nine stages that were classified depending on the following  $D_p$  values: <0.43, 0.43–0.65, 0.65–1.1, 1.1–2.1, 2.1–3.3, 3.3–4.7, 4.7–7.0, 7.0–11 and >11  $\mu\text{m}$ . The filters were changed for each disk temperature, and approximately 300 L of air was passed through the sampler when the brakes were applied 20 times under the respective conditions.

#### 2.4. Chemical analysis of metallic elements in brake pads and size-classified abrasion dusts

To determine the elemental composition of the bulk pads used for the dynamometer abrasion tests, the pads were filed using a ceramic file and then ground into powder with an agate mortar for 10 min. Approximately 1.5 mg of the powdered sample was placed into a PTFE vessel and digested by 1 mL of hydrofluoric acid (50% atomic absorption spectrometry grade, Kanto Chemical Co., Inc., Japan), 4 mL of nitric acid (60% electronic laboratory grade, Kanto Chemical Co., Inc.), and 0.5 mL of hydrogen peroxide (30% atomic absorption spectrometry grade, Kanto Chemical Co., Inc.) in a microwave digestion system (Multiwave, Anton Parr GmbH, Austria) under the condition of 700 W for 10 min and 1000 W for another 10 min. Hydrofluoric acid was evaporated by heating the sample solution at 200 °C on a hot plate, and 0.1 mol L<sup>-1</sup> of nitric acid (prepared from 60% nitric acid) was added to obtain a 50 mL sample.

The filters that contain the samples collected by the Andersen low-volume sampler were introduced into the PTFE vessel and digested by the above mentioned procedure. K, Ti and Fe were determined by an inductively coupled plasma atomic emission spectrometer (ICP-AES) (Ciros CCD, Rigaku, Japan), while Cu, Zn, Sb and Ba were determined by an inductively coupled plasma mass spectrometer (ICP-MS) (SPQ9000, Seiko Instrument Inc., Japan). Table 1 shows the analytical conditions for ICP-AES and ICP-MS.

To confirm the validity of the analytical procedures, we also measured a standard reference material of APM prepared by the NIST (National Institute of Standards and Technology) SRM 1648 (urban particulate matter). The analytical results were in good agreement with the certified values.

Table 1  
Analytical conditions for ICP-AES and ICP-MS

ICP-AES	
RF power	1400 W
Plasma Ar flow	13.0 L min <sup>-1</sup>
Auxiliary Ar flow	1.0 L min <sup>-1</sup>
Carrier Ar flow	1.0 L min <sup>-1</sup>
Nebulizer	Bavington type
Monochrometer	Paschen-Runge type
Focus length	0.5 m
Grating (for short wavelength)	2924 grooves mm <sup>-1</sup>
Grating (for long wavelength)	2400 grooves mm <sup>-1</sup>
Detector	Linear CCD array
Measurement mode	Direct reading
ICP-MS	
RF power	1300 W
Plasma Ar flow	15.0 L min <sup>-1</sup>
Auxiliary Ar flow	1.0 L min <sup>-1</sup>
Carrier Ar flow	0.7 L min <sup>-1</sup>
Sampling depth	10.0 mm
Nebulizer	Meinhard type
Mass filter	Quadrupole
Detector	Electron multiplier
Measurement mode	Peak hopping

### 3. Results and discussion

#### 3.1. Time profiles of the disk and pad temperatures

Fig. 2 shows the time profiles of the disk and pad temperatures obtained during the tests of pad C (the profiles of pads A and B were almost similar to that of pad C). When the brakes were applied once at 200 or 300 °C, the disk temperature increased by ca. 25 °C (initial speed of 50 km h<sup>-1</sup>), while at 400 °C (initial speed of 80 km h<sup>-1</sup>), it increased by ca. 45 °C; it then decreased gradually due to the air flow from the blower after the series of braking cycles. On the other hand, the pad temperature increased by ca. 5–10 °C when the brakes were applied once. This increase was less than that of the disk, and it depended on the heat capacity of the disk and the pad. From the results, it is evident that the particle size distribution measurements in this study were performed under the conditions of the precisely controlled temperature profiles.

#### 3.2. Number concentration of brake abrasion dusts

Fig. 3 shows the time profiles of the number concentration  $dN/d\log D_p$  (#/cm<sup>3</sup>) of the particles between  $D_p$  values of 1.486 and 1.596  $\mu\text{m}$ . An interesting finding is that two prominent peaks were observed when the brakes were applied once. The

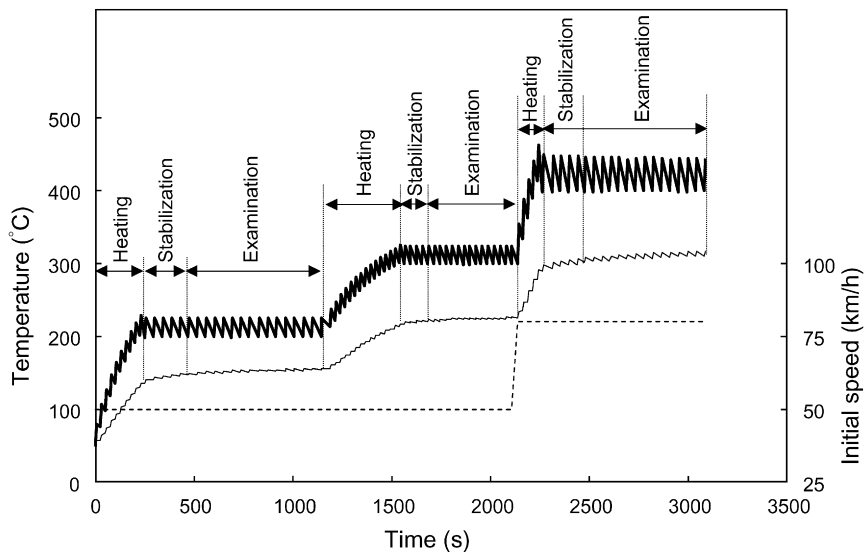


Fig. 2. Time profiles of disk and pad temperatures obtained during the measurement of particle size distribution for pad C. Y-axis on the left: the bold line (—) indicates the disk temperature and the thin line (—), the pad temperature. Y-axis on the right: the broken line (---) indicates the initial disk rotation speed.

first peak, showing a large amount of abrasion dust emission, appeared immediately after the start of braking. This peak must be due to the collision and subsequent friction between the disk and the pads. On the other hand, the second peak appeared at the restart of the idle rotation. This secondary emission is probably caused by the detachment of the abrasion dust present on the disk or the pad surfaces. The number concentration of the abrasion dust particles returns to the indoor background level after 25 s of braking. Therefore, the signal generated after 25 s from the beginning of braking is defined as the background signal. Hence, we calculate the number concentration of the particles due to individual braking cycle from the difference between the integrated signal generated during 24 s from the beginning of braking and the background signal. Since the signal levels are too low to be analyzed, probably due to the low abrasion rates or irregularity of the sampling setup for the tests of pad A at 200 or 300 °C, these results are excluded from the evaluation.

Since the measurement by using the APS were conducted in the open system, the number concentration should not be considered as the total amount of abrasion dusts. In addition, a large variation in the number concentration was observed due to the fluctuation of the air-flow rate from the cooling blower (see Fig. 3). However, it is possible to discuss whether the use of relative values depends on the

pad type or disk temperature because the tests were conducted by the same procedure. Since the initial speed was increased to 80 km h<sup>-1</sup> at 400 °C, the emission rates measured for both pads were larger than those at other temperatures. Some braking parameters such as the friction time, deceleration rate and weight of the automobile may also contribute significantly to the emission rates of the abrasion dusts, although these parameters were not examined in this study.

### 3.3. Particle size distribution of brake abrasion dusts

Fifteen particle size distributions of the abrasion dusts were obtained in each brake pad test at the disk temperatures of 200, 300 and 400 °C (except for pad A at 200 or 300 °C; see Fig. 3). For the data obtained in individual braking cycle, the number concentration classified in each particle size range is normalized by the maximum number concentration in order to eliminate the effect of the number concentration variation. Fig. 4 shows the normalized distributions of the number concentration of the abrasion dusts, and Fig. 5 shows those of the mass concentration calculated from the number concentration. All distributions of the number concentration exhibit peak values at  $D_p$  values of approximately 1–2 μm (see Fig. 4) and those of the mass concentration have peaks between  $D_p$  values of 3 and 6 μm (see Fig. 5). These results are almost

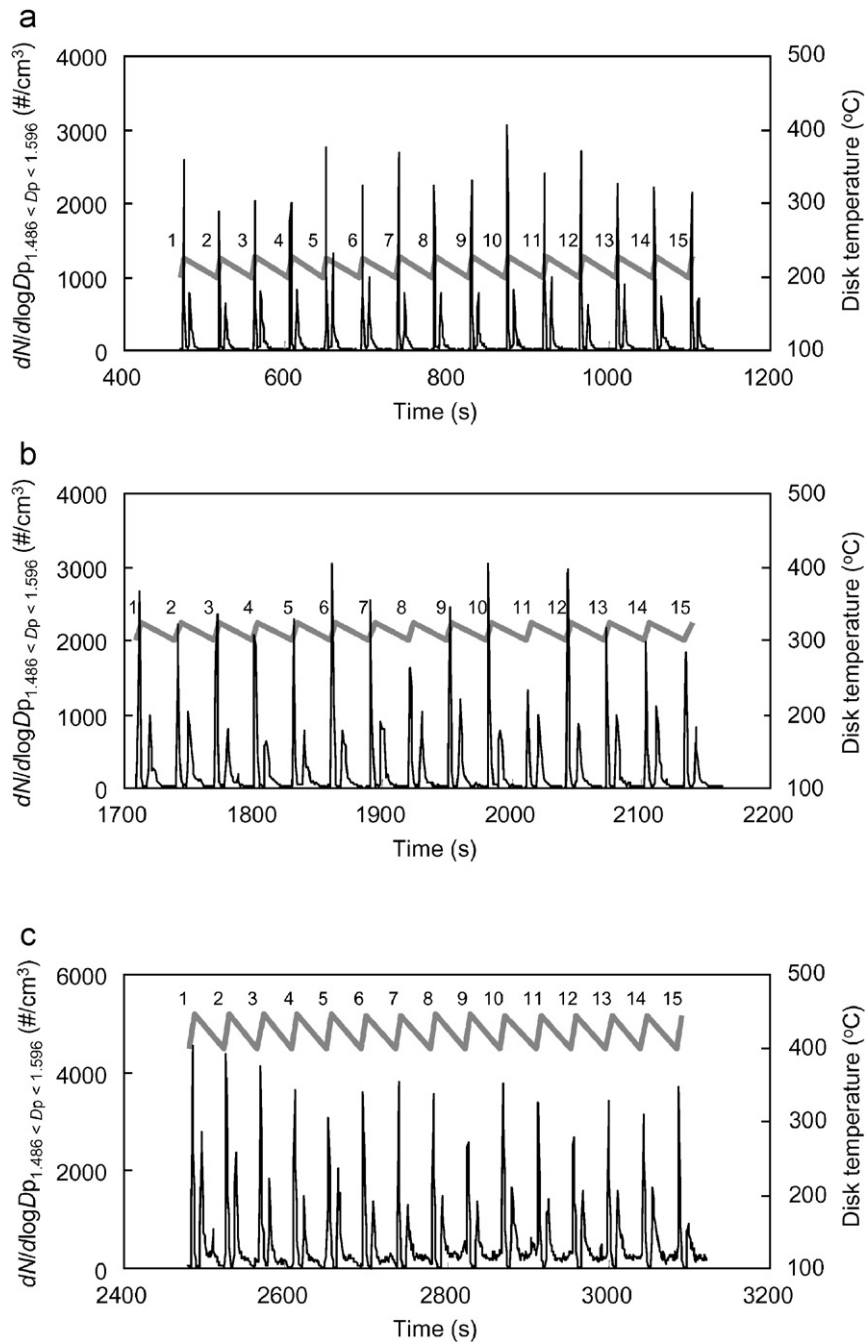
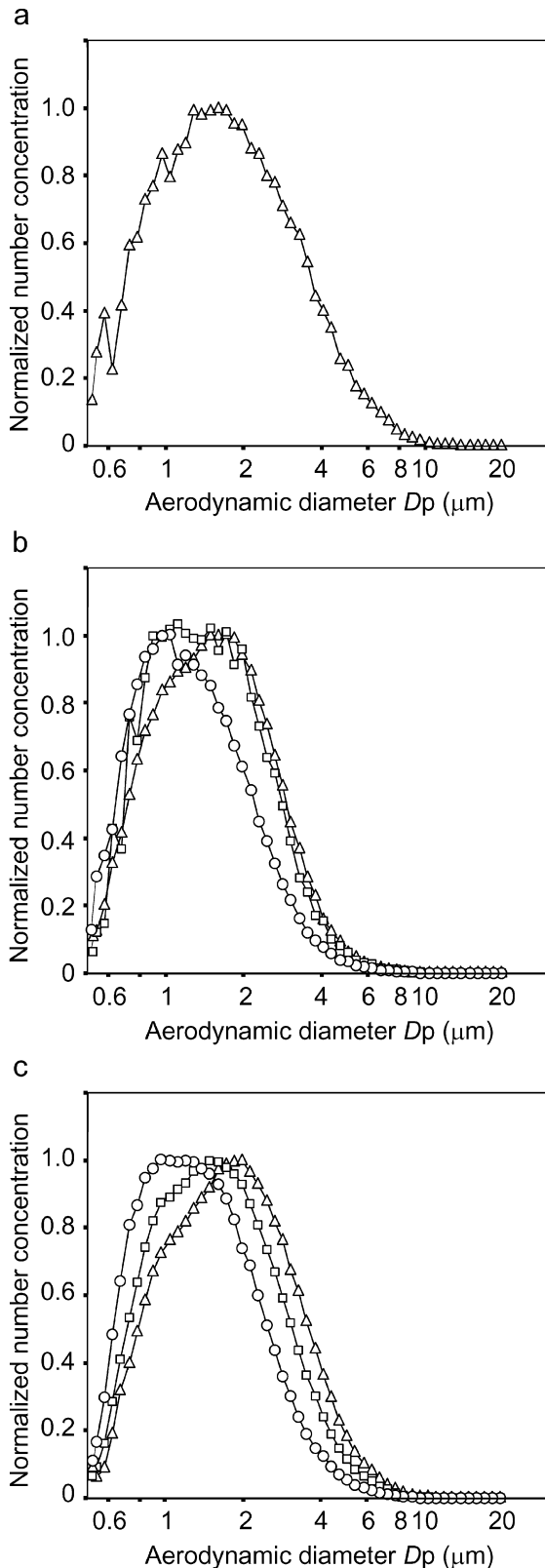


Fig. 3. Time profiles of the number concentration of particles between  $D_p$  values of 1.486 and 1.596  $\mu m$  obtained at different disk temperatures for pad C. (a), (b) and (c) show the results obtained by braking 20 times at disk temperatures of 200, 300 and 400  $^{\circ}C$ , respectively. Y-axis on the left: the thin line (—) indicates the number concentration (number  $cm^{-3}$ ) of particles. Y-axis on the right: the bold line (—) indicates the disk temperature. The number attached to the bold line indicates the serial number of the braking cycle at the each temperature.

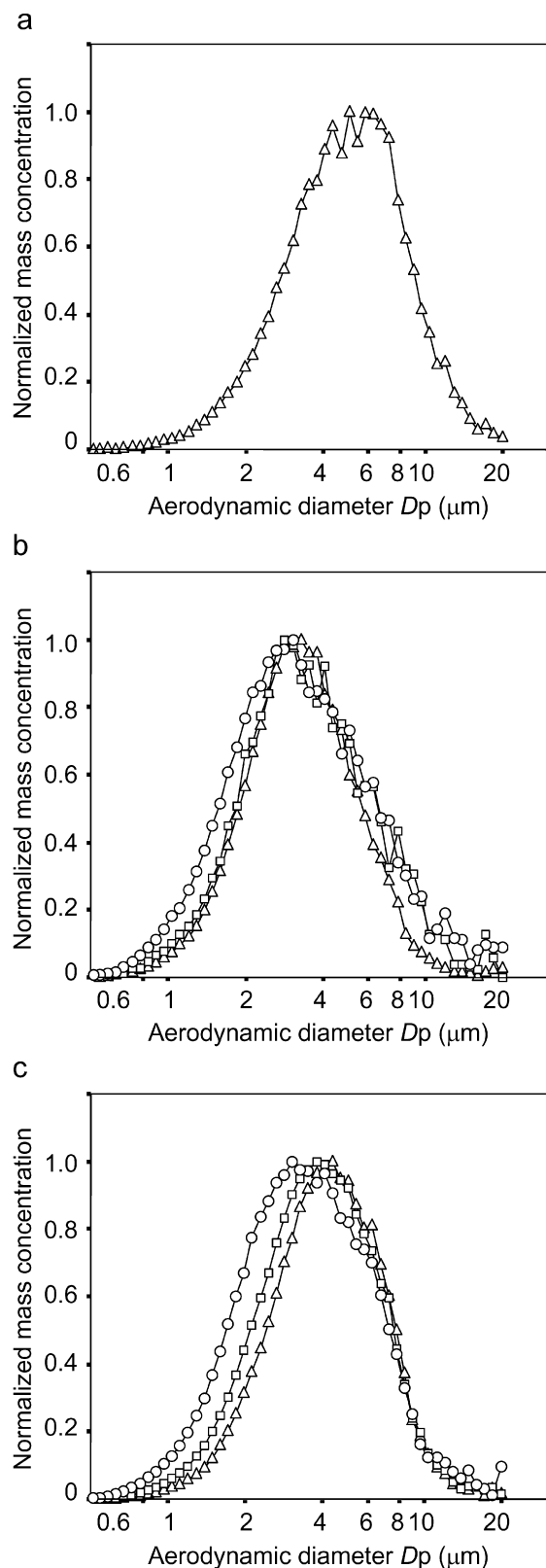
consistent with those of the previous report of Sanders et al. (2003), while they are quite different from the report of Garg et al. (2000). The measurements of Sanders et al. (2003) and those in

this study were carried out in an open system, while the measurements by Garg et al. (2000) were carried out in a closed chamber. In order to estimate the amounts of the entire abrasion dusts generated from



a brake dynamometer, the brake assembly and the sampling probes of the measurement instruments should be enclosed in a closed chamber, as adopted by Garg et al. (2000). However, in this system, the particle size distribution could deviate from the original because the particle aggregation or deposition due to the interaction between the particles and the chamber wall might occur (Tu, 2000). Therefore, the bimodal ( $D_p < 0.1$  and  $> 10 \mu\text{m}$ ) distributions obtained by Garg et al. (2000) might be different from those for the generated dusts. On the other hand, since Sanders et al. (2003) and we measured the particle size distributions in the open system, such effects will be avoided. In particular, we collected the abrasion particles from just below the brake caliper, so that the distributions exhibited in this study would be regarded as those of the original brake abrasion dusts. These results indicate that most brake abrasion dusts consist of fine particles. In addition, we should consider that the APS used in this study cannot be used to detect particles whose sizes are greater than  $D_p$  values of  $20 \mu\text{m}$ . Some of the distributions obtained by Garg et al. (2000) show a significant emission of large particles ( $D_p > 18 \mu\text{m}$ ) particles, which obviously could not be detected and calculated in this study. In the range of the particle size estimated in this study ( $D_p = 0.5\text{--}20 \mu\text{m}$ ), the peak shifts to the coarse side depending on the disk temperature during the tests of pads B or C. It is suggested that the pad matrix becomes brittle due to the reduction in the binding strength of the resin that holds the brake components together. Based on the number concentration, it is estimated that 74% ( $400^\circ\text{C}/\text{pad C}$ ) to 92% ( $200^\circ\text{C}/\text{pad B}$ ) of the abrasion dust can be emitted as PM<sub>2.5</sub> (see Fig. 4). This corresponds to 12–36% of the total abrasion dust mass (see Fig. 5). In particular, the production of fine particles is dominant (abrasion dusts with the number concentration of approximately 90% and the mass concentration of approximately 30% can be emitted as PM<sub>2.5</sub>) at the disk temperature of  $200^\circ\text{C}$ , which corresponds to the condition simulating an urban district driving. The particle size distributions of the

Fig. 4. Normalized particle size distributions of brake abrasion dusts expressed as the number concentration. (a), (b) and (c) show the distributions of the pads A, B and C, respectively. Open circles ( $-\circ-$ ), squares ( $-\square-$ ) and triangles ( $-\triangle-$ ) indicate the results obtained at 200, 300 and  $400^\circ\text{C}$ , respectively. The number concentration in the respective particle size range was normalized by the maximum concentration.



abrasion dusts observed in this study reveal that they would be one of the prominent sources of PM<sub>2.5</sub>.

### 3.4. Concentration of metallic elements in the brake pad in Japan

The metallic elements included in the brake pads are listed in Table 2. Although the compositions of the metallic elements in the brake pads are different, a few weight percent of K, Ti, Cu, Sb and Ba are included in all pads. Potassium titanate is added to brake pads to improve their heat resistance and wear characteristics (Hee and Filip, 2005). Copper fiber and barium sulfate are the major materials that control the braking characteristics such as the braking force, thermal conductivity and vibration (Chan and Stachowiak, 2004; Tang and Lu, 2004). The concentrations of Sb in the pads examined in this study are in the range of 0.712–1.67%; these values are slightly less than those of the pads generally used in European cars (Sb concentrations of 1–5%) (Weckwerth, 2001). Sb<sub>2</sub>S<sub>3</sub> acts as a lubricant to reduce excessive wear in the high-load condition (Jang et al., 2004). The relative elemental concentrations to Sb are also listed in Table 2. The relative values of K, Ti, Cu and Ba to Sb in the brake pad used in this study are in the range of 1.1–2.5, 5.1–6.5, 9.1–18 and 4.4–19, respectively. These elemental components (K, Ti, Cu, Sb and Ba) might be good indicators to distinguish brake abrasion dusts from other source particles.

### 3.5. Distribution of metallic elements included in size-classified abrasion dusts

Elemental distributions in size-classified dusts were obtained for each abrasion test. Fig. 6 shows the elemental distributions of K, Ti, Fe, Cu, Zn, Sb and Ba obtained by the abrasion test in the condition of pad C and 200 °C. The shapes of the distributions of six metallic elements (Ti, Fe, Cu, Zn, Sb and Ba) were very similar to the total mass distribution of the brake abrasion dusts shown in

Fig. 5. Normalized particle size distributions of brake abrasion dusts expressed as the mass. (a), (b) and (c) show the distributions of pads A, B and C, respectively. Open circles (—○—), squares (—□—) and triangles (—△—) indicate the results obtained at 200, 300 and 400 °C, respectively. The mass concentration in the respective particle size range was normalized by the maximum concentration.

Table 2  
Concentration<sup>a</sup> of metallic elements in brake pads studied in this report

Element	Concentration (%)					
	Pad A		Pad B		Pad C	
	Mean $\pm$ SD	Ratio <sup>b</sup>	Mean $\pm$ SD	Ratio <sup>b</sup>	Mean $\pm$ SD	Ratio <sup>b</sup>
K	4.10 $\pm$ 0.19	2.5	1.42 $\pm$ 0.05	2.0	1.81 $\pm$ 0.10	1.1
Ti	9.50 $\pm$ 0.47	5.7	4.60 $\pm$ 0.09	6.5	8.19 $\pm$ 0.43	5.1
Fe	8.55 $\pm$ 0.40	5.1	0.117 $\pm$ 0.047	0.16	0.362 $\pm$ 0.005	0.23
Cu	15.2 $\pm$ 3.2	9.1	13.0 $\pm$ 0.4	18	17.6 $\pm$ 4.5	11
Zn	0.0306 $\pm$ 0.0011	0.018	0.0695 $\pm$ 0.0191	0.098	3.18 $\pm$ 0.33	2.0
Sb	1.67 $\pm$ 0.03	1.0	0.712 $\pm$ 0.033	1.0	1.60 $\pm$ 0.11	1.0
Ba	7.27 $\pm$ 0.14	4.4	13.2 $\pm$ 0.18	19	13.1 $\pm$ 0.9	8.2

<sup>a</sup>Values obtained by analysis of three samples.

<sup>b</sup>Relative concentration to Sb; [Element]/[Sb].

Fig. 5. However, the distribution of K shows a small peak in the sub-micro range. Sub-micro size particles are supposed to be generated by the coaggregation of volatile compounds (Topping et al., 2004). Therefore, these fine particles may originate from some volatile compounds contained in K.

In order to compare the elemental composition between the bulk pads and the size-classified abrasion dusts, the relative concentrations of abrasion dusts were calculated from the data in Fig. 6 and Table 2. Fig. 7(a) shows the elemental ratios of K, Ti, Fe, Cu, Zn, Sb and Ba obtained by the abrasion test in the condition of pad C and 200 °C. The leftmost column indicates the data for bulk pad C. Large amounts of Fe are found in all size ranges of abrasion dusts, although the bulk pad C does not contain Fe. This observation suggests that a large amount of Fe-enriched abrasion dusts are derived from the cast iron disk. In order to eliminate the impact of the cast iron disk, the same elemental ratios except Fe are redrawn in Fig. 7(b). As shown in Fig. 7(b), a considerably high ratio of K is found in the sub-micro range. The probable source of K is mentioned previously. Furthermore, the same elemental ratios except Fe and K are redrawn in Fig. 7(c) in order to clarify the similarity between the elemental compositions of the bulk pads and the size-classified abrasion dusts. As shown in Fig. 7(c), a considerably high ratio of Ti is also found in the sub-micro range. From Fig. 7(b) and (c), potassium titanate ( $K_2O \cdot nTiO_2$ ), which is used to improve heat resistance and wear characteristics (Hee and Filip, 2005), is also a possible source of sub-micro particles containing K and Ti. Except sub-micro

range particles, all abrasion dusts retain the elemental ratio of the bulk pad C. Since the abrasion dusts of more than 0.65  $\mu$ m account for more than 90% of the total weight of abrasion dusts, the elemental composition of Cu, Zn, Sb and Ba is considered to retain that of the bulk pad. Elemental ratios in size-classified abrasion dusts were investigated for other experimental conditions, but significant differences from the results under the condition of pad C and 200 °C were not observed.

### 3.6. Estimation of Sb emission from brake abrasion dusts

From the results of this and our previous study (Furuta et al., 2005), it is suggested that automotive brake abrasion dusts would be one of the sources of Sb-enriched fine APM. Next, we attempt to estimate the Sb emission from automotive brake abrasion dusts. In general, the brake setup of a passenger car consists of four disk brake systems installed in all wheels or two-disk brake systems installed in the front wheels and two drum brake systems installed in the rear wheels. A pair of brake pads is set in a single-disk brake system and parts of abrasion dusts will be emitted to the ambient air in the case of the disk brake system. On the contrary, the drum brake is a closed system and hence the abrasion dust cannot be emitted outward. The amounts of abrasion dusts emitted to the ambient air are estimated based on the following assumption. The weights of friction materials per brake pad for the front and the rear brake systems are 110 and 60 g, respectively. The lifetimes defined as the period consuming 60% of the friction materials for the

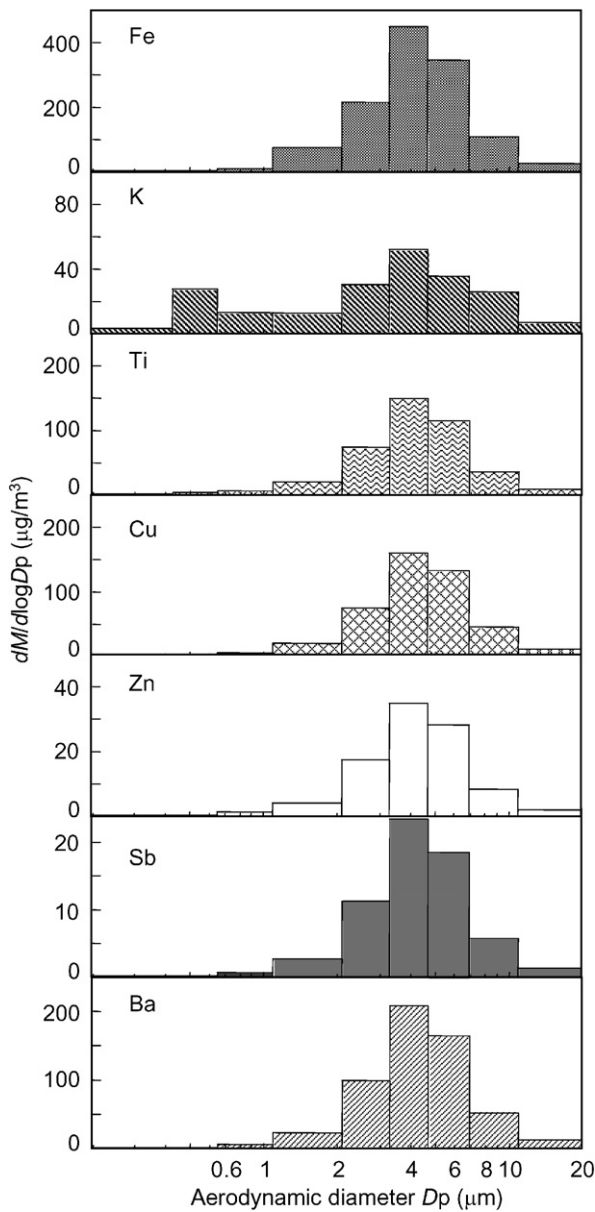


Fig. 6. Distributions of metallic elements present in size-classified brake abrasion dusts obtained by the abrasion test in the condition of pad C and 200 °C expressed as the mass concentration. ■: Fe, ▨: K, ▩: Ti, ▤: Cu, □: Zn, ■: Sb, ▥: Ba.

front and the rear systems are 5 and 7 years, respectively. Half the passenger cars have four disk brake systems, while the other half have two disk brake systems installed only in the front wheels.

The emission of brake abrasion dusts from a passenger car is estimated as 63 g car<sup>-1</sup> yr<sup>-1</sup>. However, all the dusts are not emitted to the ambient air because a fraction of dusts may deposit on the wheel surface. Garg et al. (2000) reported that 35% of the

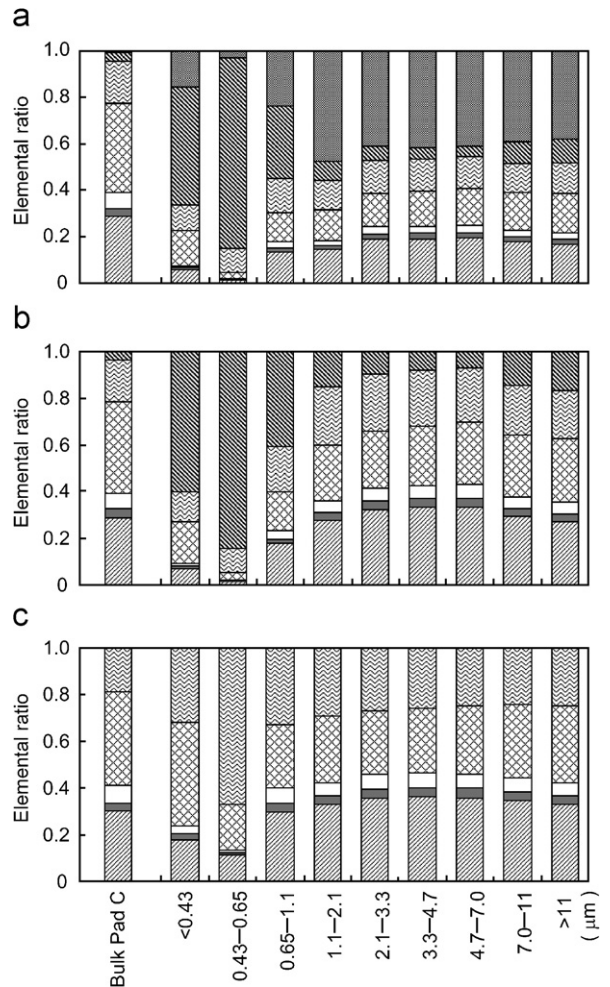


Fig. 7. Elemental ratios of bulk pad C and size-classified abrasion dusts obtained by the abrasion test in the condition of pad C and 200 °C. (a) Elemental ratios of all elements (K, Ti, Fe, Cu, Zn, Sb and Ba) measured in this study, (b) Elemental ratios except Fe. (c) Elemental ratios except Fe and K. ■: Fe, ▨: K, ▩: Ti, ▤: Cu, □: Zn, ■: Sb, ▥: Ba.

brake pad mass could be emitted to the ambient air as particles. However, this might be an underestimation because particle aggregation or deposition might occur due to the interaction with the inner wall of the closed chamber. Sanders et al. (2003) adopted the open system and estimated that 50–70% of brake wear could be emitted to the ambient air. The estimation by Sanders et al. (2003) may be relatively reasonable as compared with that of Garg et al. (2000) because the open system is similar to actual braking. Hence, when we adopt the 70% emission ratio estimated by Sanders et al. (2003), the emission of brake abrasion dusts is corrected as 44 g car<sup>-1</sup> yr<sup>-1</sup>.

The averaged Sb concentration (1.33%) of the three types of brake pads was used as the representative data of brake pads containing Sb in Japanese passenger cars. Hence, the Sb emission is calculated as  $0.59 \text{ g car}^{-1} \text{ yr}^{-1}$ . There are 55,200,000 passenger cars owned in Japan (JAMA, 2005). However, non-Sb brake pads have recently been adopted in some Japanese passenger cars. We assume that the Sb-containing brake pads account for 65% of the total pads, according to our preliminary investigation by a random sampling method. Thus, the number of passenger cars with Sb-containing brake pads is estimated to be 35,880,000, and 21 tons of Sb may be emitted to the ambient air as brake abrasion dusts from passenger cars per year in Japan. Since the Sb distribution in size-classified dusts was almost consistent with the mass distribution of abrasion dusts, it would be possible to estimate the emission of Sb as PM<sub>2.5</sub>. As mentioned previously, since approximately 30% of the brake dust produced while driving in an urban district has a particle size of less than  $2.5 \mu\text{m}$ , the amount of Sb emitted as PM<sub>2.5</sub> in Japan may be  $6.3 \text{ ton yr}^{-1}$ .

This is the first trial to estimate the Sb emission from automotive brake abrasion dusts in Japan. Correct information disclosure by a manufacturer is indispensable to grasp a more accurate estimation.

#### 4. Conclusions

Our previous study revealed that a vast majority of Sb-enriched fine APM ( $<2 \mu\text{m}$ ), and automotive brake abrasion dusts, which were suspected as one of the sources, were edgy-shaped. In addition, this study demonstrated that approximately 90% of brake abrasion dusts (on the basis of number concentration) are distributed in a small size range ( $<2.5 \mu\text{m}$ ). The shapes of the distributions of Ti, Fe, Cu, Zn, Sb and Ba were very similar to the total mass distribution of the brake abrasion dusts, and the elemental composition of Cu, Zn, Sb and Ba is considered to retain that of the bulk pad. From these results, it is concluded that automotive brake abrasion dusts containing percentage level of Sb would be one of the prominent sources of the Sb-enriched fine APM.

#### Acknowledgments

This study was supported by a grant from the New Policy Division of the Gunma Prefectural

Government, Japan. We would like to thank Kimiyo Kumagai (Gunma Prefectural Institute of Public Health and Environmental Sciences), Satoru Udagawa (Tokyo Dylec, Co.), Eiichi Yoshida, Yasuo Takagi, and Yosuke Sasaki (Akebono Brake Industry, Co., Ltd.) for providing advice and technical assistance.

#### References

- Adachi, K., Tainosho, Y., 2004. Characterization of heavy metal particles embedded in tire dust. *Environment International* 30, 1009–1017.
- Borja-Aburto, V.H., Castillejos, M., Gold, D.R., Bierzwinski, S., Loomis, D., 1998. Mortality and ambient fine particles in southwest Mexico City, 1993–1995. *Environmental Health Perspectives* 106, 849–855.
- Calcabrini, A., Meschini, S., Marra, M., Falzano, L., Colone, M., Berardis, B.D., Paoletti, L., Arancia, G., Carla, F., 2004. Fine environmental particulate engenders alterations in human lung epithelial A549 cells. *Environmental Research* 95, 82–91.
- Chan, D., Stachowiak, G.W., 2004. Review of automotive brake friction materials. *Proceedings of the Institute of Mechanical Engineers Part D* 218, 953–966.
- Furuta, N., Iijima, A., Kambe, A., Sakai, K., Sato, K., 2005. Concentrations, enrichment and predominant sources of Sb and other trace elements in size classified airborne particulate matter collected in Tokyo from 1995 to 2004. *Journal of Environmental Monitoring* 7, 1155–1161.
- Gao, Y., Nelson, E.D., Field, M.P., Ding, Q., Li, H., Sherrell, R.M., Gigliotti, C.L., Van Ry, D.A., Glenn, T.R., Eisenreich, S.J., 2002. Characterization of atmospheric trace elements on PM<sub>2.5</sub> particulate matter over the New York–New Jersey harbor estuary. *Atmospheric Environment* 36, 1077–1086.
- Garg, B.D., Cadle, S.H., Mulawa, P.A., Groblicki, P.J., 2000. Brake wear particulate matter emissions. *Environmental Science and Technology* 34, 4463–4469.
- Gomez, D.R., Smichowski, P., Gine, M.F., Sanchez-Bellato, A.C., 2005. Antimony: a traffic-related element in the atmosphere of Buenos Aires, Argentina. *Journal of Environmental Monitoring* 7, 1162–1168.
- Hee, K.W., Filip, P., 2005. Performance of ceramic enhanced phenolic matrix brake lining materials for automotive brake linings. *Wear* 259, 1088–1096.
- International Agency for Research on Cancer, 1989. *Mono-graphs on the Evaluation of Carcinogenic Risk of Chemicals to Man*. IARC, Lyons, pp. 291–305.
- Jang, H., Kim, S.J., 2000. The effects of antimony trisulfide ( $\text{Sb}_2\text{S}_3$ ) and zirconium silicate ( $\text{ZrSiO}_4$ ) in the automotive brake friction material on friction characteristics. *Wear* 239, 229–236.
- Jang, H., Ko, K., Kim, S.J., Basch, R.H., Fash, J.W., 2004. The effect of metal fibers on the friction performance of automotive friction materials. *Wear* 256, 406–414.
- Japan Automobile Manufacturers Association, Inc., 2005. *The Motor Industry of Japan 2005*. JAMA, Tokyo, p. 42.
- Kenny, L.C., Liden, G., 1991. A technique for assessing size-selective dust samplers using the APS and polydisperse test aerosols. *Journal of Aerosol Science* 22, 91–100.

- Krachler, M., Zheng, J., Shoty, W., Koe, R.R., Zdanowicz, C., Fisher, D., 2005. Increasing atmospheric antimony contamination in the northern hemisphere: snow and ice evidence from Devon Island, Arctic Canada. *Journal of Environmental Monitoring* 7, 1169–1176.
- Lim, M.C.H., Ayoko, G.A., Morawska, L., 2005. Characterization of elemental and polycyclic aromatic hydrocarbon compositions of urban air in Brisbane. *Atmospheric Environment* 39, 463–476.
- Lippmann, M., Ito, K., 2000. Contributions that epidemiological studies can make to the search for a mechanistic basis for the health effects of ultrafine and larger particles. *Philosophical Transactions of the Royal Society of London Series A* 358, 2787–2797.
- Lough, G.C., Schauer, J.J., Park, J., Shafer, M.M., Deminter, J.T., Weinstein, J.P., 2005. Emissions of metals associated with motor vehicle roadways. *Environmental Science and Technology* 39, 826–836.
- Magari, S.R., Schwartz, J., Williams, P.L., Hauser, R., Smith, T.J., Christiani, D.C., 2002. The association of particulate air metal concentrations with heart rate variability. *Environmental Health Perspectives* 110, 875–880.
- Oberdoerster, G., 2005. Effects and fate of inhaled ultrafine particles. *American Chemical Society Symposium Series* 890, 37–59.
- Pakkanen, T.A., Kerminen, V.-M., Loukkola, K., Hillamo, R.E., Aarnio, P., Koskentalo, T., Maenhaut, W., 2003. Size distributions of mass and chemical components in street-level and rooftop PM<sub>1</sub> particles in Helsinki. *Atmospheric Environment* 37, 1673–1690.
- Sanders, P.G., Xu, N., Dalka, T.M., Maricq, M.M., 2003. Airborne brake wear debris: size distributions, composition, and a comparison of dynamometer and vehicle tests. *Environmental Science and Technology* 37, 4060–4069.
- Sasaki, Y., 1994. Development of non-asbestos friction materials. In: *Proceedings of Fifth Akzo Symposium*, Konigswinter, Germany. pp. VII-1–VII-12.
- Sioutas, C., Abt, E., Koutrakis, P., Wolfson, J.M., 1999. Evaluation of the measurement performance of the scanning mobility particle sizer and aerodynamic particle sizer. *Environmental Science and Technology* 30, 84–92.
- Sternbeck, J., Sjoedin, A., Andreasson, K., 2002. Metal emissions from road traffic and the influence of resuspension: results from two tunnel studies. *Atmospheric Environment* 36, 4735–4744.
- Tang, C.-F., Lu, Y., 2004. Combinatorial screening of ingredients for steel wool based semimetallic and aramid pulp based nonasbestos organic brake materials. *Journal of Reinforced Plastics and Composites* 23, 51–63.
- Topping, D., Coe, H., Mcfiggans, G., Burgess, R., Allan, J., Alfarra, M.R., Bower, K., Decesari, S., Facchini, M.C., 2004. Aerosol chemical characteristics from sampling conducted on the Island of Jeju, Korea during ACE Asia. *Atmospheric Environment* 38, 2111–2123.
- Tu, J.Y., 2000. Numerical investigation of particulate flow behavior in particle–wall impaction. *Aerosol Science and Technology* 32, 509–526.
- Uexküll, V.O., Skerfving, S., Doyle, R., Braungart, M., 2005. Antimony in brake pads—a carcinogenic component? *Journal of Cleaner Production* 13, 19–31.
- Weckwerth, G., 2001. Verification of traffic emitted aerosol components in the ambient air of Cologne (Germany). *Atmospheric Environment* 35, 5525–5536.